# High-speed Waveguide Modified Uni-Traveling Carrier Photodiodes with 130 GHz Bandwidth


Linze Li
*School of Information Science and Technology*
*ShanghaiTech University*
Shanghai, China
lilz@shanghaitech.edu.cn

Luyu Wang
*School of Information Science and Technology*
*ShanghaiTech University*
Shanghai, China
wangly4@shanghaitech.edu.cn

Baile Chen*
*School of Information Science and Technology*
*ShanghaiTech University*
Shanghai, China
chenbl@shanghaitech.edu.cn



***Abstract*—We demonstrate evanescently-coupled waveguide modified uni-traveling carrier (MUTC) photodiodes with an external responsivity of 0.12 A/W, and a 3-dB bandwidth of 130 GHz.**



***Keywords—waveguide photodiode, high-speed photodetector, MUTC***


## I. Introduction

The development of terahertz (THz) technology has driven the demand for high-speed and high-power photodiodes (PDs). Uni-traveling carrier photodiodes (UTC-PDs) [1], with only electrons as the active carriers in the drift layer [2], are one of the most promising options for applications such as mm-wave communication and photonic microwave generation [3]. The way of optical coupling could significantly influence the performance of the UTC PDs. For surface-illuminated PDs, since the carrier transport and the optical coupling are both in the vertical direction, it is challenging to achieve short carrier transit time and high responsivity simultaneously [4]. In contrast, waveguide PDs can effectively eliminate the bandwidth-responsivity tradeoff by coupling the light laterally into the active region of the device through an optical waveguide [5]. In this work, we demonstrate an evanescently-coupled waveguide modified uni-traveling carrier (MUTC) PD with optimized high impedance coplanar waveguide (CPW) designs. The device shows a 3dB bandwidth of 130 GHz and external responsivity of 0.12 A/W.

## II. Device Structure and Fabrication

Fig. 1 (a) shows the designed epitaxial structure of the InGaAs/InP wafer. The structure was grown on the semi-insulating InP substrate. The epitaxial growth began with a total 600 nm heavily n-doped InP contact layer and a 400 nm InGaAsP waveguide layer. Then, an InP drift layer was deposited as the charge compensation layer and cladding for the waveguide, and a cliff layer was inserted in the collector to reduce the effect of space charge effect at high current levels [6]. The 180 nm thick InGaAs absorption layer consists of a depleted lightly n-doped layer and a graded doped p-type layer that form a quasi-electric field to assist electron transport. Finally, the structure was capped by a heavily p-doped InP diffusion block layer and an InGaAs contact layer. To smooth energy band discontinuities, InGaAsP quaternary layers were deposited at InGaAs/InP heterojunction interfaces.

The device was fabricated into a double-mesa structure, as shown in Fig. 1 (b). The p-mesa and the passive waveguide were formed by an inductively coupled plasma (ICP) dry etch process. The second mesa was terminated at the semi-

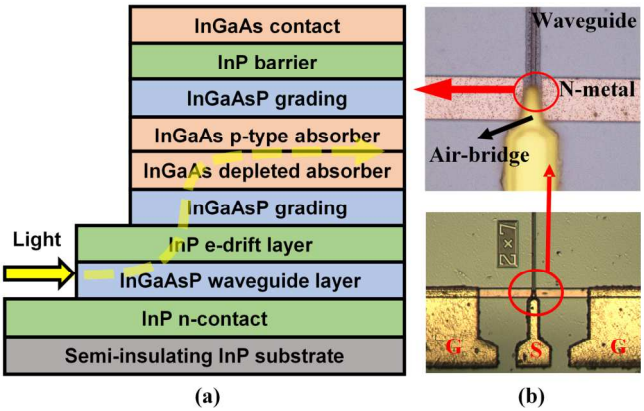


Fig. 1. (a) Epi-layer structure of the InGaAs/InP photodiode. (b) Micrograph of a fabricated device.

insulating InP substrate by wet etch ($H_3PO_4$:HCl = 1:3) to ensure electrical isolation between devices. Ti/Pt/Au/Ti and GeAu/Ni/Au were deposited on the p-type and n-type contact layers by electron beam evaporation, respectively. A good ohmic contact was formed by the rapid thermal annealing process. The photodiodes were connected to gold-plated CPW pads through an air-bridge. Apart from CPWs with 50 Ω characteristic impedance, high impedance transmission lines were also fabricated to introduce inductive peaking to improve 3dB bandwidths.

## III. Characterization

The dark current versus bias voltage characteristics for devices with active areas of 2 × 20 μm$^2$, 2 × 15 μm$^2$, 2 × 10 μm$^2$ and 2 × 7 μm$^2$ at room temperature are shown in Fig. 2. Under −5 V bias, typical dark currents are in the range of $10^{-6}$ A, which is mainly due to the surface leakage caused by dry etch process.

The frequency response of the InGaAs/InP waveguide devices was investigated by an optical heterodyne setup [7]. Two tunable lasers with wavelengths near 1.55 μm were coupled together to generate a beat signal with a frequency from hundreds of megahertz to more than 140 GHz. The modulated optical signal at 1.55 μm wavelength was coupled into the device by a lensed fiber. The measurements were conducted in two frequency ranges. From DC to 110 GHz, the RF signal was collected by the Rohde & Schwarz power meter (NRP-Z58) through the GSG Model 110H probe, while the DC bias was provided by the source meter through a 110 GHz bias tee. Frequency-dependent loss value introduced by cables, bias tee and GSG probe was calibrated by a vector network analyzer (VNA) with corresponding calibration kit (85058E & CS-5 for DC to 67 GHz, WR10-VDI & CS-5 for

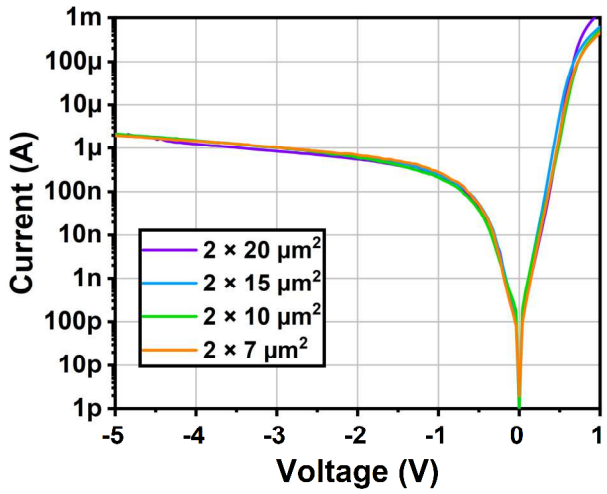


Fig. 2. Dark current versus bias voltage characteristic for devices with various areas at room temperature.

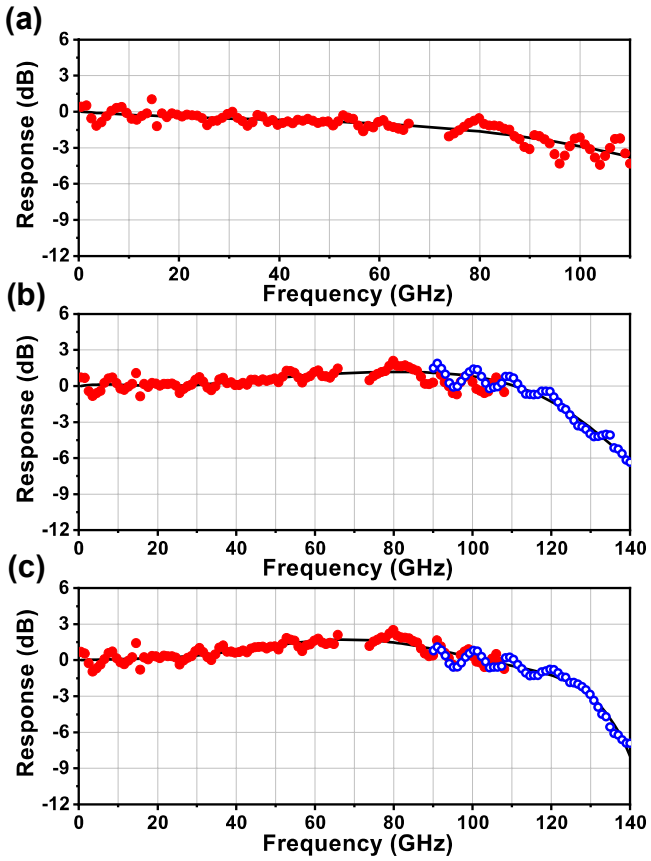


Fig. 3. Frequency response of the (a) 50 Ω load device with 2 × 10 μm² area, (b) high impedance device with 2 × 10 μm² area and (c) high impedance device with 2 × 7 μm² area under −2.5 V bias and 4mA photocurrent. (red points: data from DC to 110 GHz, blue points: data from 90 GHz to 140 GHz, solid line)

73.8 GHz to 110 GHz). From 90 GHz to 140 GHz, a GGB Model 140 waveguide probe with an integrated bias tee was used and connected to a VDI power meter (PM5). The loss file provided by the manufacturer was included in the measurement results. The external responsivity of the 2 × 7 μm² device is 0.12 A/W.

Theoretically, the 3dB bandwidth of the photodiode is limited by transit time and RC time, as expressed by the equation [8]:

$$\frac{1}{{f_{3dB}}^2} = \frac{1}{{f_{RC}}^2} + \frac{1}{{f_{tr}}^2} \quad (1)$$

where $f_{3dB}$, $f_{RC}$, $f_{tr}$ are the total 3-dB bandwidth, RC-limited bandwidth, and transit-time-limited bandwidth, respectively. Fig. 3 shows the normalized frequency response of PDs with different CPW designs under −2.5 V bias at a photocurrent of 4 mA. For the 2 × 10 μm² device with 50 Ω load, the 3dB bandwidth is 100 GHz. The 2 × 7 μm² and 2 × 10 μm² devices with high impedance CPWs show 3dB bandwidths of 130 GHz and 125 GHz respectively. The red and blue points, representing experimental data in two different frequency ranges, show good overlap from 90 GHz to 110 GHz. The high impedance transmission line incorporates an inductor into the PD circuit, resulting in a peaking effect at around 80 GHz, which greatly improves device bandwidths.

To further investigate the bandwidth limiting factor of devices, the scattering parameters (S11) of waveguide PDs were measured by VNA. Parameter fitting was conducted in Advanced Design System (ADS) software with the equivalent circuit as depicted in Fig. 4. $R_s$, $R_p$ and $C_{PD}$ represent the series resistance, junction resistance and photodiode capacitance, respectively. $C_t$ and $L_t$ denote the capacitance and inductance of the high impedance CPW, respectively.

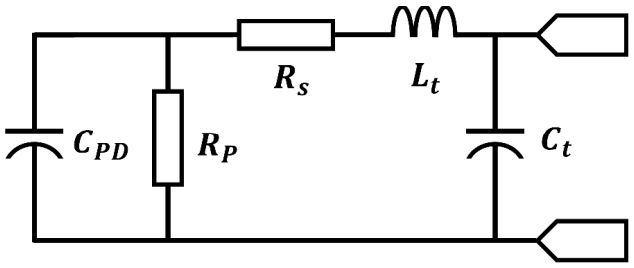


Fig. 4. Equivalent circuit model of the UTC device for S11 fitting.

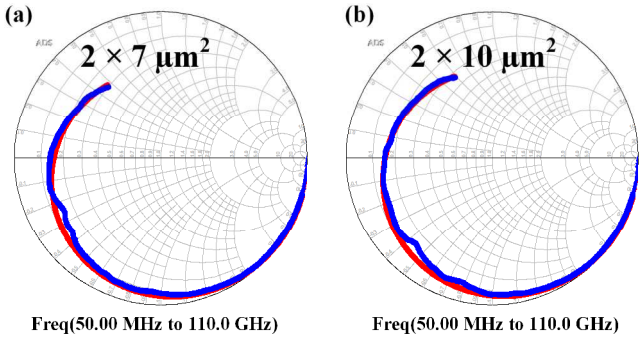


Fig. 5. Measured (blue line) and fitted (red line) S11 data of (a) 2 × 7 μm² and (b) 2 × 10 μm² devices with 50 MHz-110 GHz frequency range under −2.5 V bias.

TABLE I. FITTED PARAMETERS

| *Area (μm²)* | *Rs (Ω)* | *$C_{PD}$ (fF)* | *$C_t$ (fF)* | *Lt (pH)* |
|---|---|---|---|---|
| **2 × 7** | 7.7 | 26.1 | 21.7 | 107.2 |
| **2 × 10** | 7.6 | 28.2 | 21.7 | 105.8 |
| **2 × 15** | 7.2 | 32.2 | 20.1 | 112.7 |
| **2 × 20** | 7.0 | 36.5 | 19.5 | 114.7 |

The fitting curves and the measured S11 data in the smith chart for the 2 × 7 μm² and 2 × 10 μm² devices under −2.5 V are shown in Fig. 5. The corresponding extracted data is summarized in Table I. The fitted junction resistance ($R_p$), typically on the order of 500 MΩ, is not listed in the table. The extracted photodiode capacitance ($C_{PD}$) is composed of junction capacitance ($C_{pn}$) and parasitic capacitance ($C_{st}$). A $C_{st}$ of 20.3 fF was found by plotting the $C_{PD}$ versus device areas, determined from the intercept of the linear fit, as shown in Fig. 6. Since $C_{st}$ accounts for most of $C_{PD}$, it is the major limiting factor of RC time.

Based on the circuit model with the extracted parameters, $f_{RC}$ can be calculated, and then the theoretical $f_{tr}$ can be derived according to (1). The transit-time-limited bandwidth

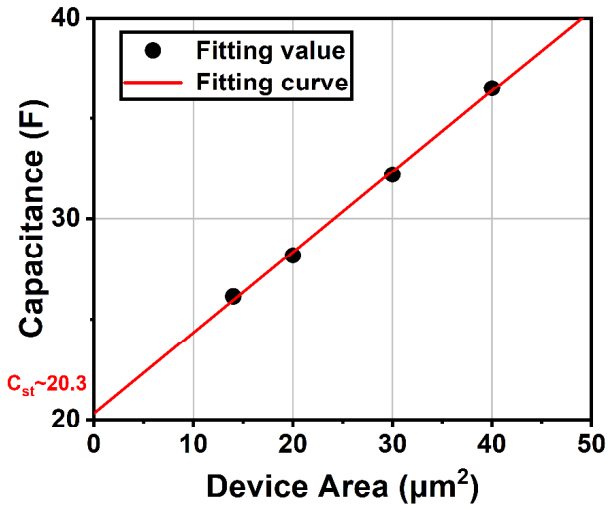


Fig. 6 Fitting capacitance of devices under −2.5 V bias and linear fit.

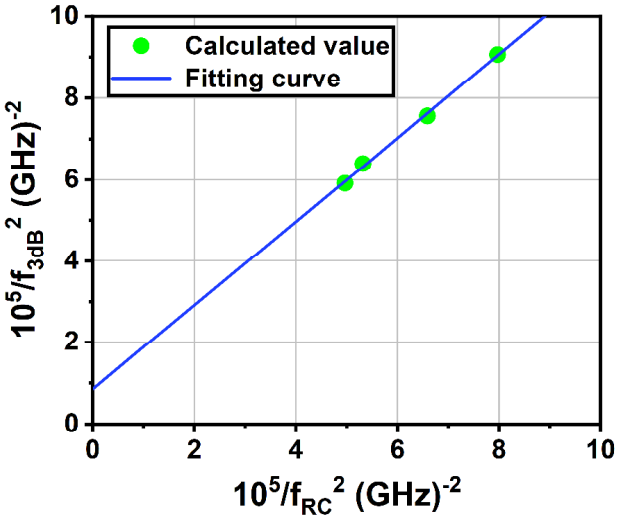


Fig. 7. Calculated $10^5/f_{3dB}{}^2$ versus $10^5/f_{RC}{}^2$ under −2.5 V bias and linear fit.

is determined to be 342 GHz from the intercept of the linear fit by plotting $10^5/f_{3dB}{}^2$ versus $10^5/f_{RC}{}^2$ (see Fig. 7). It can be observed that the bandwidth is limited by $f_{RC}$, indicating that further optimization of the fabrication process is needed to reduce the parasitic capacitance.

## IV. Conclusion

In this work, we have reported InGaAs/InP based high-speed waveguide MUTC PDs operating at 1550 nm wavelength with a responsivity of 0.12 A/W. The 3 dB bandwidths under −2.5 V bias of the 2 × 7 μm² devices reached 130 GHz with carefully designed high impedance CPW.

## Acknowledgment

This work was supported in part by the National Natural Science Foundation of China under Grant 61975121, and in part by the Double First-Class Initiative Fund of ShanghaiTech University. We are grateful for the device fabrication support from the ShanghaiTech University Quantum Device Lab.

## References

[1] T. Ishibashi, N. Shimizu, S. Kodama, H. Ito, T. Nagatsuma, and T. Furuta, *Uni-Traveling-Carrier Photodiodes*. 1997, p. UC3.

[2] T. Ishibashi, T. Furuta, H. Fushimi, and H. Ito, "Photoresponse characteristics of uni-traveling-carrier photodiodes," *Proceedings of SPIE - The International Society for Optical Engineering,* vol. 4283, pp. 469-479, 07/09 2001, doi: 10.1117/12.432597.

[3] J. P. Seddon, M. Natrella, X. Lin, C. Graham, C. C. Renaud, and A. J. Seeds, "Photodiodes for Terahertz Applications," *IEEE Journal of Selected Topics in Quantum Electronics,* vol. 28, no. 2: Optical Detectors, pp. 1-12, 2022, doi: 10.1109/JSTQE.2021.3108954.

[4] Q. Li *et al.*, "High-Power Flip-Chip Bonded Photodiode With 110 GHz Bandwidth," *Journal of Lightwave Technology,* vol. 34, no. 9, pp. 2139-2144, 2016, doi: 10.1109/JLT.2016.2520826.

[5] Q. Li *et al.*, "High-Power Evanescently Coupled Waveguide MUTC Photodiode With >105-GHz Bandwidth," *Journal of Lightwave Technology,* vol. 35, no. 21, pp. 4752-4757, 2017, doi: 10.1109/JLT.2017.2759210.

[6] Z. Li, H. Pan, H. Chen, A. Beling, and J. C. Campbell, "High-Saturation-Current Modified Uni-Traveling-Carrier Photodiode With Cliff Layer," *IEEE Journal of Quantum Electronics,* vol. 46, no. 5, pp. 626-632, 2010, doi: 10.1109/JQE.2010.2046140.

[7] Y. Chen, Z. Xie, J. Huang, Z. Deng, and B. Chen, "High-speed uni-traveling carrier photodiode for 2 μm wavelength application," *Optica,* vol. 6, p. 884, 07/20 2019, doi: 10.1364/OPTICA.6.000884.

[8] Z. Xie, Z. Zhou, L. Li, Z. Deng, H. Ji, and B. Chen, "High-Speed 850 nm Photodetector for Zero-Bias Operation," *IEEE Journal of Selected Topics in Quantum Electronics,* vol. 28, no. 2, pp. 1-7, 2022, doi: 10.1109/jstqe.2021.3095470.